Article

pubs.acs.org/Biomac

Injectable MMP-Sensitive Alginate Hydrogels as hMSC Delivery Systems

Keila B. Fonseca,[†,‡,§] David B. Gomes,[†,‡] Kangwon Lee,[∥,⊥,$] Susana G. Santos,[‡] Aureliana Sousa,[‡] Eduardo A. Silva,[⊥,#] David J. Mooney,[∥,⊥] Pedro L. Granja,[‡,§,○] and Cristina C. Barrias*[,‡]

[‡]INEB - Instituto de Engenharia Biomédica, Universidade do Porto, Rua do Campo Alegre 823, 4150-180 Porto, Portugal

[§]Departamento de Engenharia Metalúrgica e Materiais, Faculdade de Engenharia da Universidade do Porto (FEUP), Porto, Portugal

[∥]School of Engineering and Applied Sciences, Harvard University, Cambridge, Massachusetts 02138, United States

[⊥]Wyss Institute for Biologically Inspired Engineering, Cambridge, Massachusetts 02138, United States

[#]Department of Biomedical Engineering, University of California, Davis, California 95616, United States

[○]ICBAS - Instituto de Ciências Biomedicas Abel Salazar, Universidade do Porto, Porto, Portugal

[$]Korea Institute of Science and Technology (KIST)/University of Science and Technology (UST), Hwarangno 14-gil 5, Seongbuk-gu, Seoul 136-791, Korea

Supporting Information

ABSTRACT: Hydrogels with the potential to provide minimally invasive cell delivery represent a powerful tool for tissue-regeneration therapies. In this context, entrapped cells should be able to escape the matrix becoming more available to actively participate in the healing process. Here, we analyzed the performance of proteolytically degradable alginate hydrogels as vehicles for human mesenchymal stem cells (hMSC) transplantation. Alginate was modified with the matrix metalloproteinase (MMP)-sensitive peptide Pro-Val-Gly-Leu-Iso-Gly (PVGLIG), which did not promote dendritic cell maturation in vitro, neither free nor conjugated to alginate chains, indicating low immunogenicity. hMSC were entrapped within MMP-sensitive and MMP-insensitive alginate hydrogels, both containing cell-adhesion RGD peptides. Softer (2 wt % alginate) and stiffer (4 wt % alginate) matrices were tested. When embedded in a Matrigel layer, hMSC-laden MMP-sensitive alginate hydrogels promoted more extensive outward cell migration and invasion into the tissue mimic. In vivo, after 4 weeks of subcutaneous implantation in a xenograft mouse model, hMSC-laden MMP-sensitive alginate hydrogels showed higher degradation and host tissue invasion than their MMP-insensitive equivalents. In both cases, softer matrices degraded faster than stiffer ones. The transplanted hMSC were able to produce their own collagenous extracellular matrix, and were located not only inside the hydrogels, but also outside, integrated in the host tissue. In summary, injectable MMP-sensitive alginate hydrogels can act as localized depots of cells and confer protection to transplanted cells while facilitating tissue regeneration.

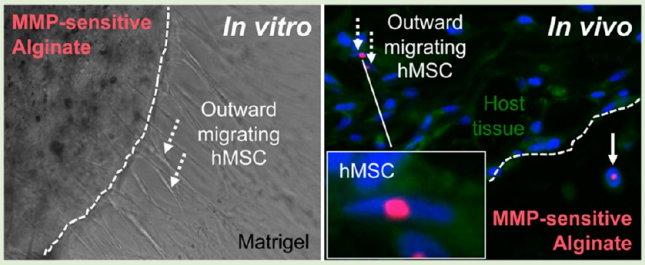

INTRODUCTION

Cell-based therapies are currently recognized as a promising approach in regenerative medicine applications. They provide cell populations that might not only secrete factors to locally modulate the activity of endogenous cells but also directly participate in the assembly of new tissue.[1] Still, the survival rates of transplanted cells are in general quite low, suggesting that improved delivery strategies are needed for increased efficacy. The use of biomaterial-based vehicles may be advantageous, as compared to dissociated-cell injection, by protecting cells from the harsh in vivo conditions, improving their viability and retention at the target site. Moreover, these cell-carriers may simultaneously act as provisional matrices to assist new tissue formation and 3D organization. Hydrogels represent an ideal class of materials for such application, as they intrinsically exhibit several extracellular matrix ECM-like features, providing cells with highly hydrated, permeable and mechanically compliant microenvironments.[2] Moreover, in situ forming hydrogels present the added benefit of injectability, which not only allows for easy cell loading and delivery, but also gives the possibility of filling-in irregular defect sites in a minimally invasive manner.[1,3−9] The importance of generating space within the hydrogel bulk in order to create spatial freedom for entrapped cells and, at a higher level, to accommodate newly forming tissues, is becoming increasingly recognized.[10,11] In their pioneer work, West and Hubbell designed a new class of cell-degradable polyethylene glycol (PEG) hydrogels, incorporating specific peptide domains that were susceptible to cellular proteases.[10] Since then, this strategy has been applied to several types of

Received: November 8, 2013
Published: December 18, 2013

   dx.doi.org/10.1021/bm4016495 | Biomacromolecules 2014, 15, 380−390

natural and synthetic polymers,[12−15] to engineer proteolytically degradable hydrogels, which represent more dynamic and physiologically relevant 3D cellular microenvironments.

We have tested a similar design to improve the properties of alginate hydrogels, as they have been and will likely continue to be one of the most important natural biomaterials used for cell entrapment.[16] In our approach, the oligopeptide sequence GGYGPVG↓LIGGK (which contains PVG↓LIG as the MMP-sensitive substrate, where the arrow represents the cleavage site), was double-end grafted to alginate chains yielding water-soluble PVGLIG-alginate conjugates.[17,18] Thus, contrary to the majority of the proteolytically degradable hydrogels described in the literature, where the protease-sensitive peptides act as main cross-linkers, these conjugates may still be easily converted into hydrogels by in situ ionic cross-linking. This increases the versatility of the system, as various peptide-modified alginates can be precombined at specific ratios, to extemporaneously prepare multifunctional hydrogels with independently tunable biochemical and viscoleastic properties. Some of the advantages of MMP-sensitive alginate hydrogels as 3D microenvironments for hMSC have been described in previous in vitro studies.[17,18] Here, we provide additional insights into the performance of these materials as cell-delivery vehicles, both in vitro and in vivo. In particular, before proceeding to in vivo studies, we started by checking the potential immunogenicity of soluble PVGLIG and PVGLIG-alginate conjugates, as measured by stimulation of dendritic cells (DC). While polymers such as alginate are reported not to lead to an adaptive immune response,[19,20] they may work as adjuvant for potentially antigenic sequences, when used as combination products, with peptides or proteins.[19] DC are the most potent antigen presenting cells (APC), responsible for surveying the body's environment, collecting antigens. Upon recognizing a pathogen or a "danger signal", DC are able to trigger an adaptive immune response, toward the encountered antigen.[19] In this context, the effect on DC maturation has been proposed as a novel biocompatibility test, to be used in combination products,[19,21] and was therefore selected for our studies. We further analyzed, in vitro, the ability of MMP-sensitive alginate hydrogels to promote outward migration and invasion of entrapped hMSC into a tissue mimic, a relevant feature for their application as cell delivery vehicles. Finally, as a proof of concept, we validated the effect of the proposed alginate modification in vivo. We implanted hMSC-laden MMP-sensitive alginate subcutaneously in a xenograft mouse model (SCID-severe combined immunodeficiency mice), using MMP-insensitive alginate hydrogels as controls. In parallel, we investigated the interplay between the hydrogels biochemical and biophysical properties, by analyzing the effect of MMP-sensitive alginate when incorporated into softer versus stiffer hydrogel matrices, prepared using different alginate concentrations.

MATERIALS AND METHODS

Alginate Samples and Molecular Weight Determination. Ultrapure sodium alginates PRONOVA LVG and VLVG (hereafter designated HMW, high molecular weight, and LMW, low molecular weight alginate, respectively) with a high guluronic acid content (68 and 67%, respectively) were purchased from Novamatrix, FMC Biopolymers. The HMW alginate was partially oxidized to a theoretical 1% molar fraction using sodium periodate, as previously described.[22,23] Average MW of alginate samples were quantified by multiple-detection size exclusion chromatography (SEC). Analyses were performed at room temperature (RT) using a modular system, composed of an automated solvent/sample delivery unit (GPCmax, Viscotek) a viscometer/right angle laser light-scattering (RALLS) dual detector (T60, Viscotek) and a refractive index detector (K-5002, Knaeur). Separations were performed in a set of three PL aquagel−OH MIXED 8 μm columns (Polymer Laboratories) with guard column, using as mobile phase 0.1 M $NaNO_3$ with 0.02 wt % NaN_3, at a flow-rate of 1.0 mL/min. Samples were dissolved in the mobile phase and prefiltered (0.2 μm) before injection. All samples were assayed in triplicate. Data were analyzed with the OmniSEC software (version 4.6.2, Viscotek).

Chemical Synthesis of Peptide-Grafted Alginate. The MMP-sensitive peptide sequence GGYGPVG↓LIGGK (abbreviated as PVGLIG) and the cell-adhesion peptide sequence GGGGRGDSP (abbreviated as RGD) were custom-made at GenScript (U.S.A.). The peptides were covalently coupled to LMW and HMW alginate, respectively, by aqueous carbodiimide chemistry using *N*-hydroxysulfosuccinimide (sulfo-NHS, Pierce) and 1-ethyl-(dimethylaminopropyl)-carbodiimide (EDC, Sigma), as previously described.[24] The peptide-grafted alginates were washed by dialysis (MWCO 3500 membrane, Spectrumlabs) against distilled water and saline, filtered (0.2 μm), freeze-dried, and stored at −20 °C until used. The grafting efficiency was calculated using the bicinchoninic acid (BCA). Total protein assay (Pierce) and the amount of double-end grafted PVGLIG were caculated using fluorescamine (Sigma), as previously described.[17] The final amounts of grafted peptides were 35 mg of PVGLIG per gram of LMW alginate, and 10 mg of RGD per gram of HMW alginate.

In Vitro Analysis of PVGLIG and PVGLIG-Alginate Conjugates Immunogenicity. Primary human monocytes were isolated from buffy coats (BC) from healthy donors (kindly donated by Instituto Português do Sangue, IPS), as previously described.[25] Briefly, after BC centrifugation (20 min, 1200*g*, RT, no brake), the peripheral blood mononuclear cell layer was collected and incubated 20 min with RosetteSep human monocyte enrichment kit (StemCell Technologies SARL) according to manufacturer's instructions. The mixture was then diluted 1:1 in phosphate buffered saline (PBS) with 2% v/v FBS (Lonza), layered over Histopaque-1077 (Sigma) and centrifuged as before. The monocyte fraction was collected, washed in PBS, and resuspended in complete medium (CM: RPMI1640 with Glutamax supplemented with 1% penicillin G-streptomycin (both from Invitrogen) and 10% v/v FBS), before cell counting using trypan blue (Sigma). Cells were >70% positive for the monocyte lineage marker Cluster Differentiation (CD) 14, and no other population was detected, in agreement with our previous results.[25] Monocyte-derived immature DC were differentiated for 6−7 days in CM, supplemented with 50 ng/mL Interleukine (IL)-4 and Granulocyte Macrophage−Colony Stimulating Factor (GM-CSF, both from Immunotools)[26,27] before incubation for 24 h with soluble PVGLIG (0.001 to 1 μM) or PVGLIG-alginate conjugates (0.5 μM PVGLIG), or 50 ng/mL lipopolysaccharide (LPS) as positive maturation control.[25,28,29] DC were harvested, washed, resuspended in staining buffer (PBS with 2% v/v FBS and 0.01 wt % NaN_3) and labeled for 45 min at 4 °C in the dark, with the following antibodies: anti-CD1a*PE and *APC, anti-CD86*FITC, anti-human leukocyte antigen (HLA)-DR*PE, antimouse immunoglobulin (Ig)G*FITC (all from Immunotools), anti-CD83*FITC (AbD Serotec), anti-HLA-A, B, C (clone W6/32) from culture supernatant (kind gift from Prof. Simon J. Powis, University of St Andrews, U.K.). Isotype matched controls were used to define background staining. Cells were washed with staining buffer and analyzed in a Fluorescence Activated Cell Sorter (FACS) Calibur (BD Biosciences), with CellQuest software. Data analysis was performed in FlowJo software. Mean fluorescence intensity (MFI) values were calculated subtracting the respective isotype controls.

Preparation of Peptide-Modified Alginate Hydrogels. Hydrogel-precursor solutions with a bimodal MW composition were prepared by combining HMW alginate (modified or not with RGD) and LMW alginate (modified or not with PVGLIG) at a 1:1 volume ratio, and a final polymer concentration of 1, 2, 3, or 4 wt %. To adjust the final amounts of each peptide independently of the total polymer concentration unmodified and peptide-modified alginates were combined at different ratios, then dissolved overnight (ON) in 0.9 wt % NaCl (Sigma), and later on mixed with an aqueous suspension of $CaCO_3$ (Fluka) and a fresh solution of δ-gluconolactone (GDL, Sigma)

dx.doi.org/10.1021/bm4016495 | *Biomacromolecules* 2014, 15, 380−390

to trigger hydrogel formation. The Ca^{2+}/COO^{-} molar ratio was set at 0.36 and the Ca^{2+}/GDL molar ratio was set at 0.5, as previously described.[17,18] The hydrogel-precursor solutions were immediately loaded into a QGel 3D disc caster and allowed to cross-link at RT.

Physicochemical Characterization of Alginate Hydrogels. The microstructure of hydrogels with different alginate concentrations was analyzed using cryogenic scanning electron microscopy (cryoSEM). Briefly, hydrogel samples were frozen in N_2 and mechanically fractured to expose their internal structure. Samples were then sublimed at −95 °C within a cryostat chamber and coated with gold/palladium. Finally, they were transferred to the cryoSEM microscope chamber (JEOL JSM 6301F/Oxford INCA Energy 350/Gatan Alto 2500) for analysis.

The rheological properties of the hydrogels were analyzed by oscillatory shear rheometry (Kinexus Pro rheometer, Malvern), using a cone-on-plate (0.5°/40 mm) geometry. Each gel-precursor solution was prepared and immediately poured on the plate for analysis. A solvent trap filled with water was used to minimize sample drying. The evolution of the shear moduli, G' (storage, elastic component) and G'' (loss, viscous component), was recorded at 20 °C as a function of time. A frequency of 1 Hz and a strain of 1% (2, 3, and 4 wt % alginate) or 5% (1 wt % alginate) were applied in order to maintain the linear viscolastic regime (LVR). The assays were run until reaching a plateau in G', and the gelling time for each formulation was determined at the crossover point ($G' = G''$). Three replicates were used for each condition.

The viscoelastic properties of preformed hydrogels were analyzed by dynamic mechanical analysis (DMA, TRITEC2000B, Triton Technology). Hydrogels were casted as discs (1.5 mm height, 6.8 ± 0.3 mm diameter) and pre-equilibrated ON at 37 °C in Dulbecco's Modified Eagle Medium (DMEM, Gibco) with 25 mM HEPES (Sigma) and 0.01 wt % NaN_3 (Sigma) at pH 7.5. Samples were kept in this solution until analysis to avoid dehydration. Viscoelastic properties were measured under unconfined compression at 1 Hz and 1% strain (within the LVR) for 5 min. A small preload was used to promote an adequate contact between the hydrogel samples and the apparatus surfaces. Results are reported in terms of compressive storage modulus (E', elastic component) and compressive loss modulus (E'', viscous component). At least five replicates were analyzed for each condition.

Culture of hMSC and Preparation of hMSC-Laden Alginate Hydrogels. Human hMSC were purchased from Lonza (PT-2501, Lot No. 6F4392) and were grown in MSCGM (hMSC growth medium, Lonza) in a humidified incubator (37 °C, 5% v/v CO_2) incubator. The medium was changed twice a week and cells were trypsinized before reaching 70% of confluence. To obtain cell-laden 3D matrices, hMSC were carefully mixed with gel-precursors solutions (2 or 4 wt % alginate) at a final density of 15×10^6 cells/mL. Hydrogel discs were casted for 1 h at RT. Matrices with a volume of 10 μL (1.5 mm height, 1.9 mm diameter) were used for in vitro studies, and matrices with a volume of 85 μL (1.5 mm height, 8.5 mm diameter) were used for in vivo studies. MMP-insensitive hydrogels were prepared with 130 μM of RGD, while MMP-sensitive hydrogels were prepared with 130 μM RGD and 325 μM of PVGLIG.

In Vitro Outward Migration and 3D-Invasive Ability of Hydrogel-Entrapped hMSC. MMP-sensitive and MMP-insensitive alginate hydrogel matrices laden with hMSC were embedded within a Matrigel layer (Becton Dickinson), incubated in complete medium and cultured under standard conditions. Three replicates were analyzed per each condition. After 3 and 7 days, phase-contrast microscopy (Axiovert 200 M, Zeiss) was used to image hMSC outward migration from the alginate hydrogel and invasion into the surrounding Matrigel layer. At day 7, cells extending outward from the hydrogel periphery were counted using The Image Analysis Count tool of Adobe Photoshop CS6 software and divided by the perimeter of the hydrogel disc, as determined using ImageJ software (http://rsb.info.nih.gov/ij/). Individual cell length was measured using ImageJ. Cells located at the alginate−Matrigel interface were imaged by confocal laser scanning microscopy (CLSM). At day 7, samples were fixed for 20 min in 4% v/v paraformaldehyde (PFA, Sigma) permeabilized in 0.1% v/v Triton X-100 (Sigma) for 5 min, and blocked for 30 min in 1 wt % bovine serum albumin (BSA, Merck) in Tris-buffered saline with calcium (TBS-Ca, pH 7.4: 50 mM Tris, 150 mM NaCl, 5 mM $CaCl_2$, all from Sigma). F-actin was stained with 40 U/mL Alexa Fluor 488 phalloidin (Invitrogen-Molecular Probes) and nuclei were counter-stained with 1 μg/mL DAPI (4′,6-diamidino-2-phenylindole). Whole-mounted constructs were imaged in a Leica SP2AOBS microscope. Final panels were assembled using Photoshop CS6.

In Vivo Studies: Subcutaneous Implantation of hMSC-Laden Alginate Hydrogels in SCID Mice. *Surgery.* All animal experiments were conducted following protocols approved by the Ethics Committee of Harvard University (Boston, U.S.A.). Mice were housed at 22 °C with a 12 h light/dark cycle and had ad libitum access to water and food. Six weeks old SCID male mice (CB17SC-M, Taconic, Germantown, NY, U.S.A.) were used as recipients. The animals were anesthetized by isofluorane inhalation, and anesthesia was maintained over the course of surgery by continuous isofluorane delivery. The dorsal surgical sites were shaved and sterilized. Single incisions were made and subcutaneous pockets were created for the insertion of hMSC-laden hydrogel discs. Four groups were tested: PVGLIG/RGD-alginate (MMP-sensitive) or RGD-alginate (MMP.insensitive), at 2 or 4 wt % alginate. Two implants were placed in each mouse and eight mice were randomly assigned to each condition. After implantation, incisions were closed with sutures and analgesics were administrated (0.05 mg Buprenorphine HCl per kg). The animals were routinely monitored for general appearance, activity, and healing of the implant sites and were euthanized after 4 weeks for implants retrieval. No mice were lost during the study.

Histology. The harvested samples, which included the entire hydrogel discs and some surrounding tissue, were fixed ON in 10% v/v neutral-buffered formalin and processed for paraffin embedding and sectioning onto slides (3 μm) using standard histological procedures (mass histology, Worcester, MA). Tissue sections were stained with Hematoxylin and Eosin (HE, Sigma), Masson's Trichrome (MT, Sigma, hematoxylin was used as counter stain), and Safranin-O/light-green (Sigma, hematoxylin was used as counter stain). The histological assessment of HE-stained sections was carried in a blinded-fashion, by nine independent evaluators. One section per sample, corresponding to a transversal section of the central part of the disc was analyzed. Images were organized so that the two gels implanted in each mouse could be directly compared in the same panel. The evaluators were asked to select from about 300 randomly organized images (corresponding to 8−10 images at 10× and 40× magnification per implant, from a total of 8 implants per group) 50% in which the degree of host tissue invasion was higher. The histology score generated by this analysis represents the relative level of tissue invasion for the different samples (PVGLIG/RGD-alginate vs RGD-alginate and 2 wt % vs 4 wt %). This scoring process was also performed using whole-section images obtained after Mosaix-reconstruction (inverted microscope, Axiovert 200 M, Zeiss). For the analysis of alginate degradation, Safranin-O/Light-Green-stained sections ($n = 4$ mice, 3 sections per mouse) were used. For each image (7 images per section), the total area of the implant was first delineated and images were analyzed and processed using MeVisLab software (Fraunhofer MEVIS, Bremen, Germany) in order to quantify the partial areas of residual alginate (% orange area) versus degraded alginate (substituted by invasion tissue, % blue/green area). Results are presented as average % of degraded alginate.

Immunohistochemistry. For human nuclei (HuNu) detection, masked epitopes were exposed by treatment with 10 mM sodium citrate (pH 6) for 35 min at 95−98 °C. Sections were incubated ON (4 °C) with mouse antihuman nuclei primary antibody (MAB4383−3E1.3 Millipore, 1:400), then with mouse-on-mouse biotinylated antimouse IgG (MOM Kit Vector, 1:1000) for 10 min at RT, and finally with Alexa Fluor 555-streptavidin (Invitrogen-Molecular Probes, 1:200) for 30 min at RT. Expression of type I collagen was probed after antigen recovery with 10 mM Tris/1 mM EDTA (pH 9) for 30 min at 95−98 °C. Sections were incubated ON (4 °C) with rabbit anticollagen I primary antibody (ab21285 Abcom, 1:100). Afterward, Alexa Fluor 594-labeled goat antirabbit IgG (Invitrogen-Molecular Probes, 1:1000) was used as the secondary antibody (1 h, RT). All sections were mounted in Fluorshield with DAPI (Sigma). Control sections for each immunolabeling excluded primary antibody staining. For tracking and quantifying hMSC, HuNu-immunolabeled sections ($n = 4$ mice, 2 sections per mouse) were used. From each section, 5−6 images were obtained,

including the whole disc periphery. In each image, the total amount of HuNu+ cells per unit area was counted, and the percentage of HuNu+ cells inside and outside the hydrogel was calculated. Results are presented as the average % of HuNu+ cells present outside the hydrogel.

Statistics. Statistical analyses were performed using GraphPad Prism 5.0 software version 5.0a. The nonparametric Mann−Whitney test was used to compare two groups, whereas comparison between more than two groups was performed using the Kruskal−Wallis test followed by Dunn's comparison test. A value of $P < 0.05$ was considered statistically significant.

RESULTS

Physicochemical Characterization of Alginate Hydrogels. Ultrapure alginate hydrogels with a bimodal molecular weight (MW) composition of high MW (HMW, $M_w = 1.5 \times 10^5$ Da) and low MW (LMW, $M_w = 2.5 \times 10^4$ Da) alginate, with different total polymer concentrations were used. The morphological cryoSEM images provided in Figure 1A do not reflect the actual mesh size of the hydrogels, which have pores in the nanometer scale. However, the images clearly show that, in terms of structure, hydrogel networks became denser as the alginate concentration increased, as expected.

Oscillatory rheometry measurements (Figure 1B) showed that increasing the alginate concentration from 1 to 4 wt % decreased the time needed to reach both the crossover point (onset of gelation) and a plateau in terms of G' (shear storage modulus) and G'' (shear loss modulus) values. Moreover, the magnitude of both moduli increased as the alginate wt% increased. DMA analyzes of preformed swollen alginate hydrogels under unconfined compression (Figure 1C) showed that a 2-fold increase in the polymer concentration (from 2 to 4 wt %), resulted in a 5-fold increase in terms of E' (compression storage modulus). Overall, all the tested hydrogel formulations exhibited a predominantly elastic behavior, with E' significantly higher than E'' (compressive loss modulus).

In Vitro Immunogenicity of PVGLIG and PVGLIG-Alginate Conjugates. To investigate the potential immunogenicity of the designed MMP-sensitive peptide sequence, we used in vitro differentiated primary human monocyte-derived DC and analyzed their activation by the peptide alone or conjugated to alginate chains, both in soluble form. As illustrated in Figure 2, presence of PVGLIG did not induce cell surface expression up-regulation of characteristic surface markers of DC maturation. While LPS (positive control) induced strong DC activation, as demonstrated by significant up-regulation of activation marker CD83, the presence of PVGLIG showed fluorescence intensity values for CD83 similar to the negative control and, for some peptide concentrations, significantly different to those obtained with LPS. The costimulatory molecule CD86, involved in the crosstalk between DC and T lymphocytes,[30] was also up-regulated upon LPS stimulation, albeit not significantly. Nonetheless, presence of PVGLIG led to CD86 surface expression similar to control levels and again, for some peptide concentrations, significantly different from LPS stimulation. The antigen presenting molecules of the major histocompatibility complex (MHC) classes I and II (HLA-A, B, C, and HLA-DR, respectively)[31] show high levels of expression, even for unstimulated DC controls, and no significant up-regulation in any of the conditions tested.

In Vitro Outward Migration and 3D-Invasive Ability of Hydrogel-Entrapped hMSC. To analyze MMP-sensitive alginate hydrogels ability to promote the outward migration and invasion of entrapped hMSC, cell-laden hydrogel matrices, Figure 3A, were embedded in a tissue mimic (Matrigel) for one week. MMP-insensitive matrices were used as a control. As depicted in Figure 3B,C, the radial migration of hMSC from 2 wt % alginate hydrogels was already detected after 4 days of culture, being more predominant in MMP-sensitive than in MMP-insensitive hydrogels. These differences were more pronounced at day 7. In Figure 3D, F-actin staining revealed the organized cytoskeleton of hMSC located at the external surface of the

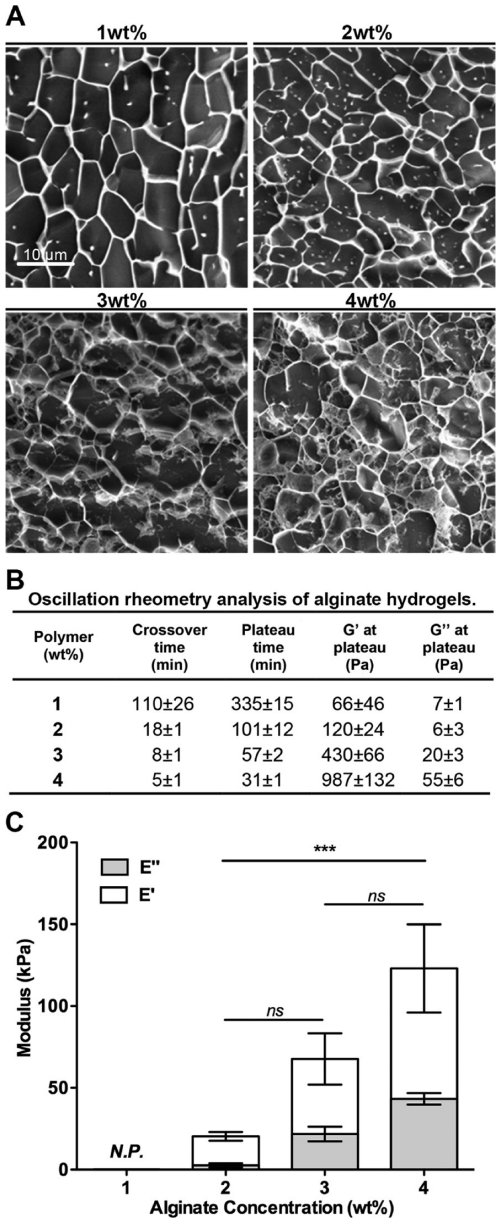

Polymer (wt%)	Crossover time (min)	Plateau time (min)	G' at plateau (Pa)	G'' at plateau (Pa)
1	110±26	335±15	66±46	7±1
2	18±1	101±12	120±24	6±3
3	8±1	57±2	430±66	20±3
4	5±1	31±1	987±132	55±6

Figure 1. Physicochemical properties of alginate hydrogels with different polymer concentrations (1, 2, 3, and 4 wt % alginate). (A) cryoSEM images showing that networks got denser as alginate wt% increased. (B) Oscillation rheometry analysis of alginate hydrogels: the gelling time decreased and the shear moduli increased as the alginate wt % increased. (C) DMA analysis of swollen alginate hydrogels under unconfined compression. Results are depicted as mean ± SD (standard deviation). Both the storage (E', elastic component) and loss (E'', viscous component) moduli increased as alginate wt% increased. All samples were predominantly elastic ($E' \gg E''$). N.P. denotes samples that were not possible to analyze by this technique (1 wt % alginate hydrogels). ***Denotes statistically significant difference ($p < 0.001$) between 4 wt % and 2 wt % groups ($n = 5$); ns denotes not statistically significant differences.

dx.doi.org/10.1021/bm4016495 | Biomacromolecules 2014, 15, 380−390

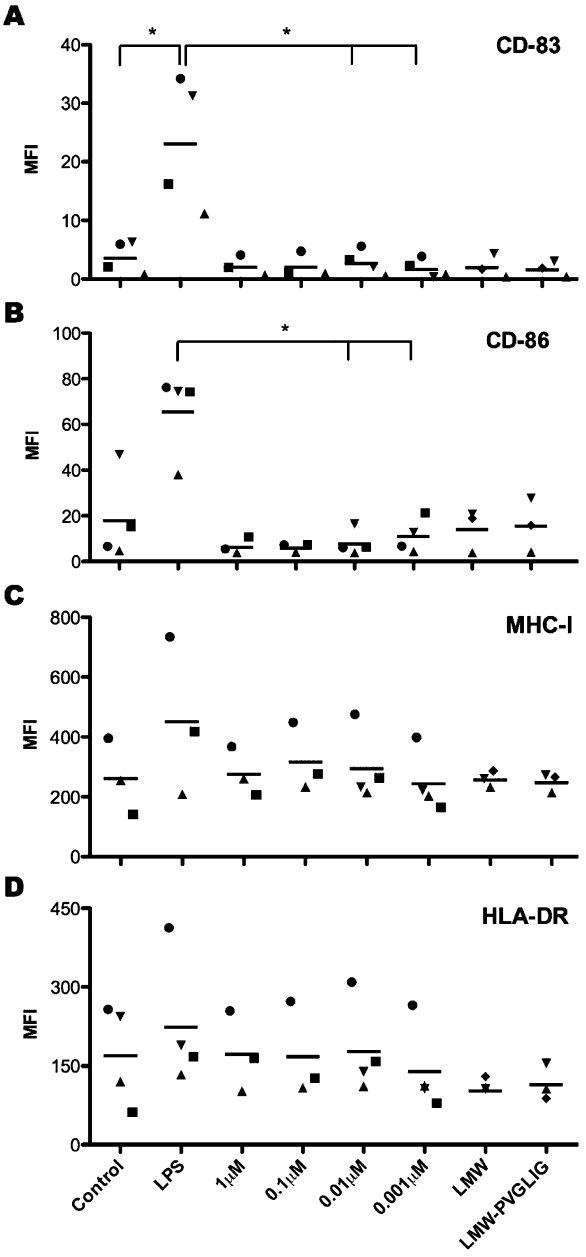

Figure 2. Flow cytometry analysis of DC activation upon exposure to soluble PVGLIG or PVGLIG-alginate conjugates. DC were either left unstimulated (negative control), stimulated with LPS (positive control), or treated with increasing concentrations of free PVGLIG or soluble PVGLIG-alginate conjugates (LMW-PVGLIG). Unmodified alginate was also used as a control (LMW). After 24 h, cells were surface-labeled with antibodies for: (A) CD-83, (B) CD-86, (C) HLA-DR, and (D) MHC-I. Each symbol represents a different donor and dashes represent the mean values. n = at least 3 independent experiments (biological replicates). *Denotes statistically significant difference ($p < 0.05$) between two groups.

hydrogels (alginate−matrigel interface). Figure 3E,F clearly show that more hMSC were able to migrate from MMP-sensitive matrices, and invade the surrounding Matrigel layer. This was quantitatively analyzed by computing the average number and extension length of outwardly migrating hMSC, which are depicted in Figure 3G. Cell migration from 4 wt % matrices was not observed, even for MMP-sensitive matrices.

In Vivo Studies with hMSC-Laden Alginate Hydrogels: Host Tissue Invasion and Hydrogel Degradation. After characterizing the in vitro behavior of hMSC-laden MMP-sensitive alginate hydrogels, we selected a xenograft mouse model to perform a first evaluation of their performance in vivo. hMSC-laden hydrogels of different compositions were implanted subcutaneously in SCID mice, and matrix remodeling was evaluated after 4 weeks, when samples still presented sufficient structural integrity to be recovered. Host tissue infiltration and alginate degradation were evaluated by histology. Analysis of HE-stained sections (Figure 4) revealed significant differences in terms of host tissue invasion of MMP-sensitive versus MMP-insensitive and 2 wt % vs 4 wt % alginate hydrogels. Figure 4A illustrates the overall morphology of explants, showing whole-section reconstructed images, while Figure 4B depicts higher magnification images, where host tissue invasion can be examined in more detail. The graphs presented in Figure 4C, show that MMP-sensitive hydrogels (P/R-alg) were more efficiently invaded by host tissue than MMP-insensitive hydrogels (R-alg), regardless of alginate content (2 wt % vs 4 wt %). In both cases, 4 wt % matrices led to considerable less host cell invasion than 2 wt % matrices.

The level of alginate hydrogels degradation/disintegration was evaluated in Safranin-O/light-green-stained sections (Figure 5A). Safranin is a basic stain that strongly binds to the negatively charged alginate matrix, providing a high contrast orange staining against the surrounding tissue (green) and, thus, an easy identification of alginate hydrogels. While in the 2 wt % groups, specimens generally comprised numerous small fragments of residual alginate, surrounded by host tissue; in the 4 wt % groups, specimens remained largely intact, with occasional alginate fragmentation into large islands. Nonetheless, in both groups, alginate degradation was more pronounced in MMP-sensitive hydrogels, as can be concluded from the quantitative analysis presented in Figure 5B.

Identification of Transplanted hMSC at the Implant Site by Immunolabeling. Transplanted hMSC were distinguished from mouse cells by immunolabeling using a monoclonal antibody specific for human nuclei (HuNu), previously validated in vitro (Figure S1A). As depicted in Figure 6, several HuNu-positive cells (HuNu+) were still present at the recipient site 4 weeks after transplantation, both inside (at the center and periphery) and outside (integrated within the host tissue) of the 2 wt % hydrogels. The presence of HuNu+ hMSC outside the 2 wt % hydrogels, which exhibited a more spindle-like shape, could be detected in all formulations, but it was more significant in 2 wt % MMP-sensitive hydrogels, as illustrated in the graph. On average, HuNu+ hMSC represented 18.5 ± 4.8% (mean ± SEM) of cells per unit area in MMP-sensitive hydrogels (P/R-alg), and 6.6 ± 1.9% in MMP-insensitive hydrogels (R-alg). A few HuNu+ hMSC could also be detected outside the 4 wt % hydrogels (Figure S1B), but they were more rare and their quantification did not yield consistent results.

ECM Production by Host and Transplanted Cells and Implant Vascularization. The deposition of new ECM at the implant site, mainly by host cells, was detected by MT-staining (Figure 7A) that clearly showed the presence of collagen (blue) around the implant. While in the stiffer 4 wt % hydrogels collagen deposition was mainly restricted to the hydrogel-host interface, in the softer 2 wt % hydrogels the new collagenous matrix appeared more uniformly distributed throughout the implant area, around the hydrogel leftovers. Expression of collagen type I by hMSC was detected in all the formulations (Figure 7B),

dx.doi.org/10.1021/bm4016495 | Biomacromolecules 2014, 15, 380−390

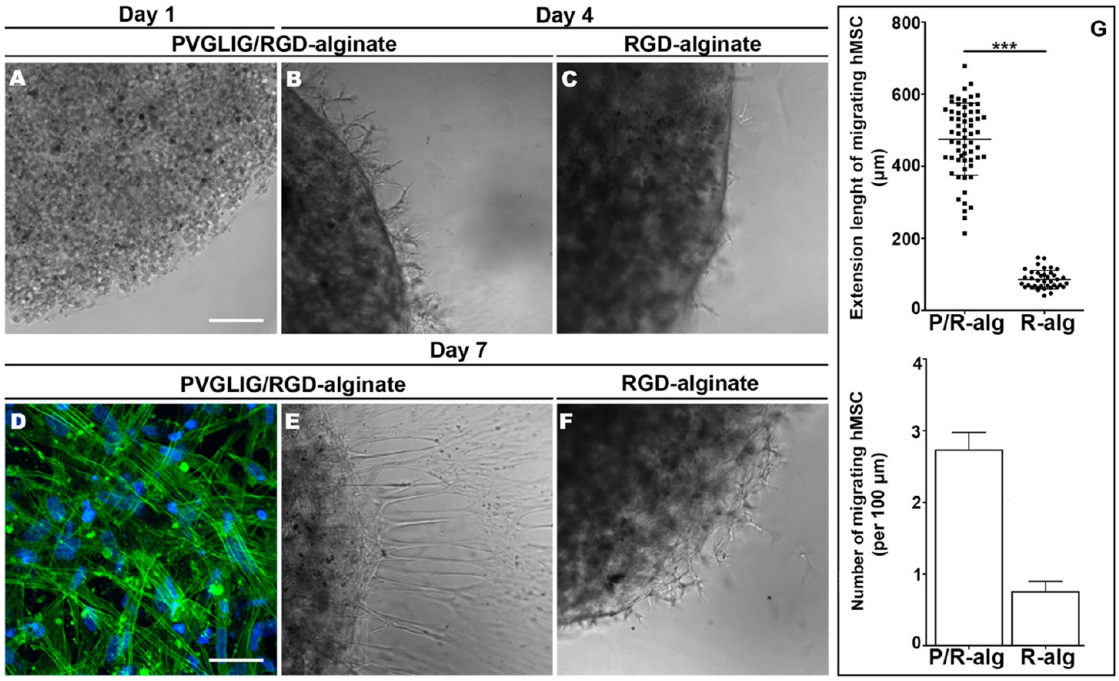

Figure 3. In vitro outward migration and 3D-invasive ability of hydrogel-entrapped hMSC. (A–F) Representative images of hMSC-laden hydrogel discs embedded in Matrigel showing (A) hMSC entrapped in 2 wt % alginate hydrogels at day 0; and hMSC migrating from the hydrogels and invading the surrounding Matrigel after (B, C) 4 days and (E, F) 7 days of culture. (D) At day 7, hMSC located at the surface of PVGLIG/RGD-alginate discs (alginate/Matrigel interface) exhibited spread morphology and an organized cytoskeleton (CLSM image of Alexa Fluor 488 phalloidin-labeled F-actin, in green; Similar results were obtained with RGD-alginate hydrogels). Scale bars: 200 μm (A–C, E, F) and 50 μm (D). (G) At day 7, hMSC extending outward the periphery of 2 wt % MMP-sensitive (P/R-alg) and MMP-insensitive (R-alg) alginates hydrogels were counted and plotted against the perimeter of the hydrogel disc (lower panel). Bars represent the average number of migrating cells per each 100 μm of perimeter and error bar represents SEM (standard error of the mean). Each dot in the upper panel graph shows individual cell length values. Mean and SD are also represented.

mainly intracellularly but also in the pericellular space, indicating that transplanted cells were able to produce their own ECM. Perfused blood vessels were detected at the implant site (Figure 7B, arrows) in all the formulations, mainly located within the newly formed tissue and at the hydrogels' periphery. Blood vessels were also sporadically detected within the hydrogels, but only in 2 wt % matrices.

DISCUSSION

Alginate hydrogels intrinsically present a number of features that make them very attractive to be used as injectable cell-depots in regenerative medicine strategies. To improve their properties as 3D cellular microenvironments, we incorporated MMP-sensitive PVGLIG motifs in alginate hydrogels,[17,18] rendering them partially degradable by cellular proteases. We hypothesized that MMP-sensitive alginate hydrogels would facilitate the in situ delivery of transplanted cells, while facilitating host tissue invasion, and potentially promoting more robust healing in vivo.

We have previously demonstrated that the viscoelastic properties of the hydrogels can be tuned independently of the peptide composition.[18] Here, we showed that a wide range of viscoleastic properties could be obtained, simply by changing the total polymer concentration in hydrogels. In view of a clinical application, such versatility is very useful as it will allow to design alginate matrices that recreate soft to moderately stiff mechanical environments, similar to those found in different kinds of native tissues.[32]

Before proceeding to in vivo experiments, we investigated the potential immunogenicity of the PVGLIG peptide, which had not been assessed before. When APC encounter small peptides, in an immunogenic context, such as in the presence of an adjuvant, a specific adaptive immune response may be triggered, as demonstrated in anticancer vaccine studies.[33] As DC are the most potent APC, the effect of combination products on their maturation is being proposed as a novel biocompatibility test for these systems.[19,21] This led us to investigate if the peptide per se or in combination with alginate could trigger DC maturation, by evaluating cell surface expression of molecules involved in activation, antigen presentation and costimulation on DC.[25] The results presented here indicate low immunogenicity of PVGLIG, free or conjugated to alginate chains. The data showed that neither of the forms induced DC maturation, as illustrated by significantly lower expression levels of CD83 and CD86, when compared with LPS-matured DC (positive control). In the current study we focused on the potential of degradation products, like free peptide or peptide coupled to alginate, to be immunogenic. Although we cannot exclude that peptide incorporated into the solid alginate hydrogels could lead to a different response by DC, previous work by Babensee and co-workers had described alginate films as not triggering DC maturation,[21] or up-regulating only some activation markers.[20] So, as the results presented here showed no DC activation, we did not proceed to investigate the effect of PVGLIG in cross-linked alginate hydrogels, where it would be considerably less accessible for presentation by DC.

In our prior studies, we showed that hMSC entrapped within MMP-sensitive (PVGLIG/RGD) alginate hydrogels were able to spread and form interconnected multicellular networks, but remained essentially round and individually dispersed in the MMP-insensitive (RGD) counterparts.[17] Here, hMSC-laden 3D matrices were embedded in Matrigel, used as a tissue mimic, and we further demonstrated that MMP-sensitive hydrogels

dx.doi.org/10.1021/bm4016495 | *Biomacromolecules* 2014, 15, 380–390

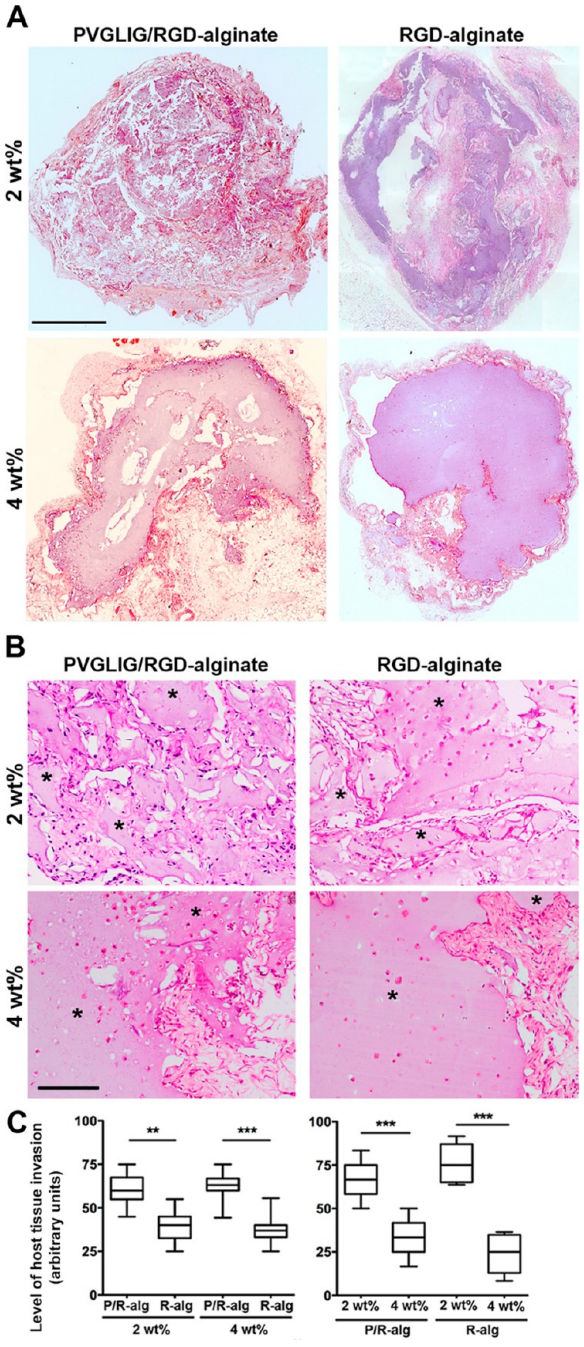

Figure 4. In vivo host tissue invasion of hMSC-laden alginate hydrogels as a function of matrix composition. (A) Representative images of transversal sections of whole discs in HE-stained slides (scale bar: 1 mm). (B) Higher-magnification images of HE-stained sections (*denotes alginate, scale bar: 200 μm) showing that host tissue invasion (pink-red) was higher in MMP-sensitive (P/R-alg) vs MMP-insensitive hydrogels (R-alg), regardless of the alginate wt%; and it was also higher in 2 wt % vs 4 wt % hydrogels, regardless of the peptide composition. (C) The extent of host tissue invasion for the different hydrogel formulations is depicted as Box and Wiskar plots, where 1−99% range is displayed and horizontal lines in each box represent median values for each condition. It was evaluated using a blind test with n = 9 independent observers. **Denotes statistically significant differences (p < 0.01); ***denotes statistically significant differences (p < 0.001).

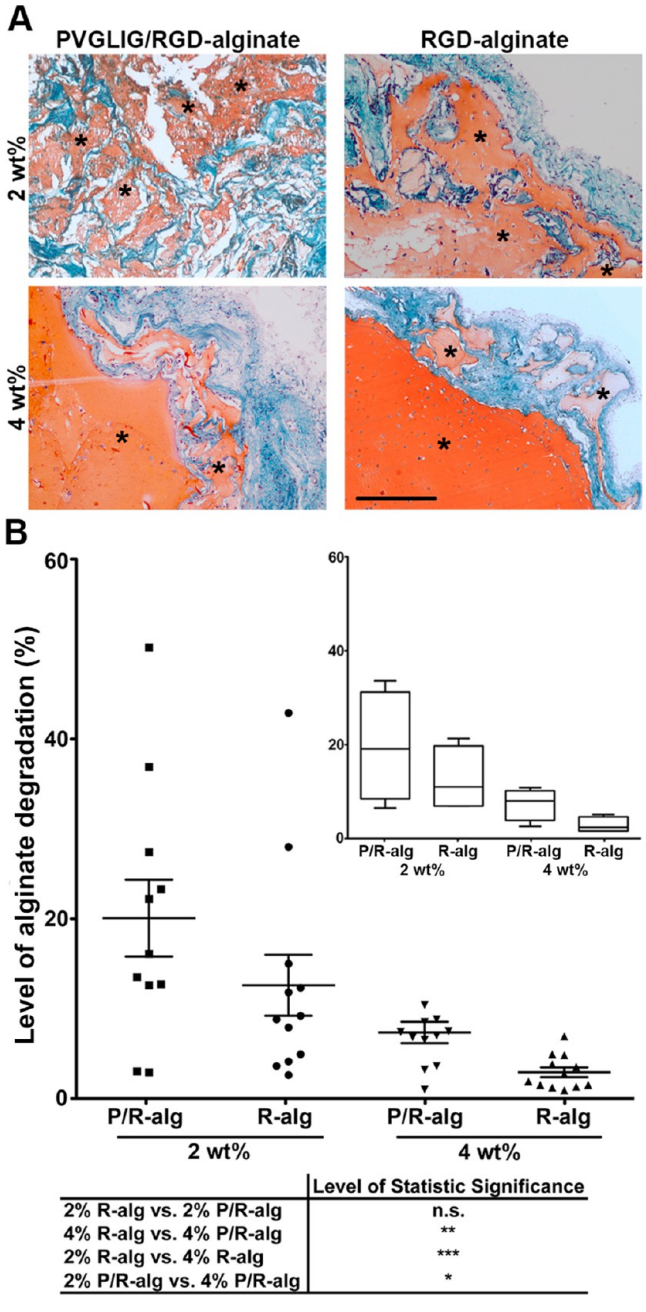

Figure 5. In vivo degradation of hMSC-laden peptide-alginate hydrogels as a function of matrix composition. (A) Representative images of Safranin-O/light-green-stained tissue sections showing a more evident fragmentation of alginate discs (in orange) in MMP-sensitive (P/R-alginate) than in MMP-insensitive hydrogels (R-alg), regardless of alginate wt%. Alginate degradation was also higher in 2 wt % vs 4 wt % matrices (green, host tissue; purple/black, nuclei; *denotes alginate; scale bar: 400 μm). (B) For the analysis of alginate degradation level, images were analyzed and processed using MeVisLab software. Results are represented in the scatter plot, where each dot represents the degradation value calculated for each single slide; mean values and SEM for each set of values are also presented. Inset: graphical representation of the results calculated per mice (n = 4) depicted in a Box and Wiskar plot, where 1−99% range is displayed and horizontal lines in each box represent median values for each condition.

facilitated the outward migration of entrapped hMSC in vitro and promoted their invasive ability. While hMSC remained essentially retained within the 2 wt % MMP-insensitive hydrogels, and only cells present at the periphery were able to escape, in 2 wt % MMP-sensitive hydrogels the enzymatic cleavage of PVGLIG motifs contributed to the destabilization of

dx.doi.org/10.1021/bm4016495 | Biomacromolecules 2014, 15, 380−390

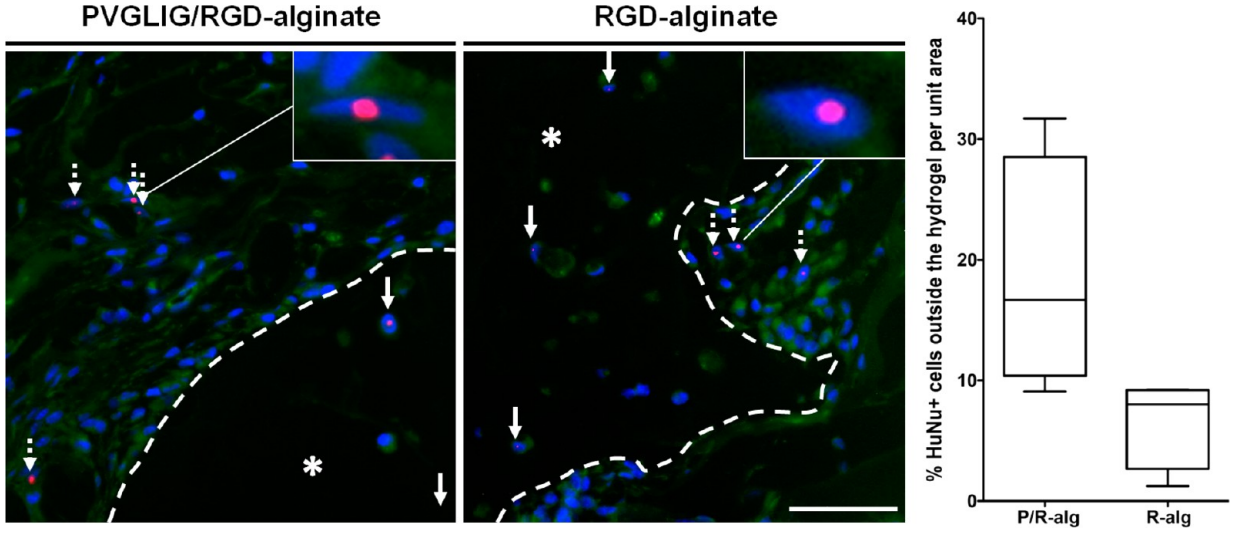

Figure 6. Identification of hMSC at the implant site. (A) Representative images of tissue sections immunostained with a human-nuclei (HuNu) specific antibody, showing HuNu+ cells (in red) inside (filled arrows) and outside (dashed arrows) 2 wt % alginate hydrogels (*denotes alginate). Dashed lines delineate the alginate hydrogels periphery (implant/host tissue interface). Nuclei are stained with DAPI (in blue), and cells present some autofluorescence (in green). Scale bar: 50 μm. The percentage of HuNu+ hMSC outside of the alginate hydrogels, in relation to the whole hMSC population, was calculated. Graphical representation of the results obtained is depicted as Box and Wiskar plots, displaying the 1−99% range, and the horizontal line in each box represents the median value for each condition.

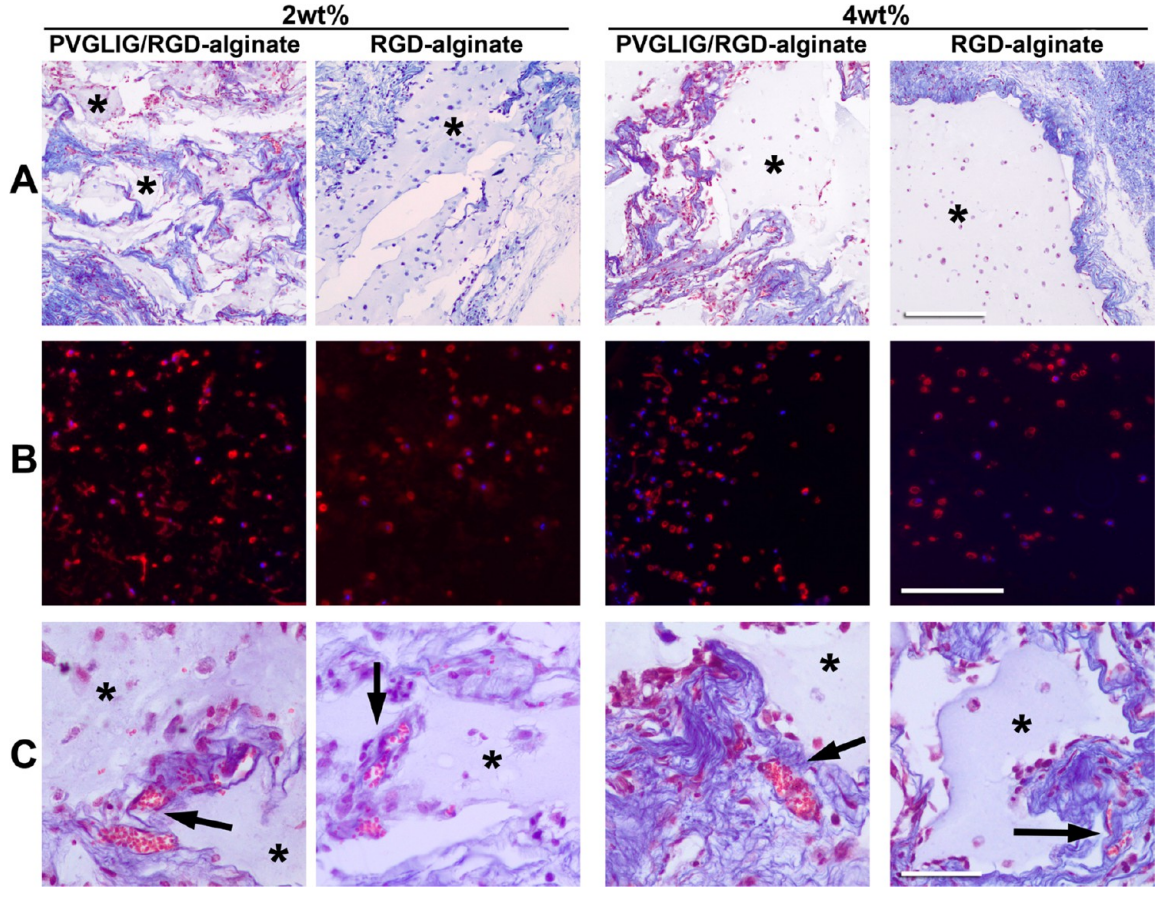

Figure 7. New ECM production and vascularization at the implant site. (A) MT-staining of collagen fibrils (blue) around the alginate hydrogel (pale blue *: alginate; light red: cell's cytoplasm; dark brown: nuclei; scale bar: 500 μm). (B) Immunostaining of collagen type I expression (red) by entrapped hMSC. Scale bar: 200 μm. (C) Identification of perfused blood vessels (arrows) at the implant site, in MT-stained sections (pale blue *: alginate; red: erythrocytes; scale bar: 50 μm).

the polymeric network, facilitating cell outward migration. Moreover, the presence of PVGLIG in MMP-sensitive hydrogels is known to stimulate the proteolytic activity of entrapped hMSC, particularly increasing secretion of active MMP-2,[17,18]

dx.doi.org/10.1021/bm4016495 | *Biomacromolecules* 2014, 15, 380−390

which certainly assisted the migrating cells in degrading and invading the surrounding Matrigel layer.

To analyze the performance of hMSC-laden MMP-sensitive alginate hydrogels in a more complex in vivo setting, we selected a xenograft mouse model for short-term subcutaneous implantation. The alginate matrices used as controls have been previously demonstrated to biodegrade or disintegrate in vivo, but by cell-independent mechanisms. More precisely, we used calcium-cross-linked ionic hydrogels, which slowly disintegrate in vivo due to the gradual substitution of Ca^{2+} by nongelling ions such as Na^{+} and Mg^{2+}.[34] The tested hydrogels had a bimodal molecular weight distribution (LMW and HMW, 1:1), which additionally contributes to the destabilization of the hydrogels,[35] and the HMW fraction was oxidized to create acetal-like groups in uronate residues, leaving it susceptible to hydrolysis.[22] Importantly, herein we were able to provide in vivo experimental evidence that the incorporation of MMP-cleavable PVGLIG motifs clearly accelerated degradation/disintegration of alginate hydrogels via a cell-driven mechanism and, thus, prove the additional effect of the proposed modification. As demonstrated before, the PVGLIG peptide can be enzymatically cleaved by MMP-2, MMP-9, MMP-13, and MMP-14.[18,36] In our past studies, MMP-2 and MMP-14 were considered to play a key role in the in vitro remodeling of MMP-sensitive alginate hydrogels, as MMP-9 and MMP-13 were not detected in the hMSC secretome.[18] However, an in vivo implantation scenario represents a much more complex proteolytic environment. Under such circumstances, the implanted matrices get in contact with multiple cell polulations, namely, with inflammatory cells that not only produce high amounts of MMPs, including MMP-9, but also secrete several cytokines and growth factors known to stimulate MMP-9 secretion by hMSC.[37] Thus, when compared to the results observed under well-controlled in vitro conditions, the mechanisms that underlined cell-driven matrix degradation in vivo are certainly more intricate and should be further investigated in the future.

The overall outcome in terms of system's performance was also influenced by the viscoelastic properties of the hydrogels. In vitro and in contrast to softer matrices (2 wt %), stiffer matrices (4 wt %) led to almost negligible hMSC outward migration along one week of culture. The stiffer matrices (4 wt %) were mainly surface-eroded, and were much less degraded than the more compliant ones (2 wt %). Yet, the effect of MMP-sensitive motifs in accelerating matrix degradation was also observed, even if less pronounced. Other authors have previously demonstrated that even in matrices susceptible to proteolytic breakdown, an increase in the matrix stiffness results in a higher physical impediment to cells, affecting diverse cellular activities.[38,39] In particular, Ehrbar et al. have recently investigated the behavior of PEG-entrapped preosteoblasts as a function of matrix biochemical and biophysical properties, and showed that the matrix stiffness was an important determinant of cell invasion in vivo.[39] Cell spreading and migration were impaired in stiffer matrices (2.5 wt %), even when those were MMP-sensitive, while cell migration was facilitated in softer hydrogels (1.5 wt %), even if the MMP activity was inhibited.[39]

The transplanted hMSC were labeled with a human-specific antibody to probe their spatial distribution at the implant site. Our results demonstrated that MMP-sensitive hydrogels facilitated the outward migration of transplanted hMSC, in agreement with our in vitro findings, behaving as more efficient cell delivery vehicles. Some of the transplanted hMSC where found outside the hydrogels, in close proximity with host cells, and thus available to more actively participate in the assembly of new tissue. In all the tested hydrogel formulations, the transplanted hMSC were able to produce their own ECM (collagen type I), which is essential to provide them structural support and replace the artificial matrix as it degrades. Given that collagen type I is a marker of osteogenic differentiation, this observation additionally suggests that entrapped hMSC were eventually differentiating along the osteoblastic lineage. However, differentiation will require further confirmation by evaluating the expression of other lineage-specific markers. The presence of numerous vessels at the implant site was also an important finding, as neo-vascularization is crucial for tissue regeneration, namely, in therapeutic strategies involving cell transplantation. Most likely, the transplanted hMSC contributed to that process by secreting pro-angiogenic factors.[40]

The utility of cell carriers is transversal to a variety of pro-regenerative therapies, intended for different kinds of tissues and pathological conditions, which will certainly present different requirements in terms of material degradation time frame. Here we provided a proof-of-concept on the ability to tune the cell-driven degradation of alginate hydrogels, through incorporation of protease-sensitive domains. In view of a specific application, it will be possible to gain additional control over the degradation process, not only by varying the percentage of cleavable motifs in the matrix, but also by designing specific peptide moieties to target particular proteases or cell types.

■ CONCLUSIONS

In summary, partial cross-linking of alginate with MMP-sensitive PVGLIG peptides offers a suitable strategy for rendering alginate hydrogels degradable by a cell-driven mechanism. This feature may improve the performance of alginate hydrogels as ECM-like vehicles for hMSC delivery in regenerative therapies, by facilitating cell release and synchronizing matrix degradation with new tissue formation. The kinetics of hydrogel degradation, and consequently of cell release, can in addition be modulated by changing the viscoelastic properties of alginate matrices. In fact, as expected, softer matrices degraded faster in vivo than stiffer matrices, irrespective of their biochemical composition (MMP-sensitive vs MMP-insensitive), but the presence of MMP-sensitive residues consistently accelerated the degradation process.

■ ASSOCIATED CONTENT

Supporting Information

Additional images are provided. This material is available free of charge via the Internet at http://pubs.acs.org.

■ AUTHOR INFORMATION

Corresponding Author

*Tel.: + 351 226074982. E-mail: ccbarrias@ineb.up.pt.

Author Contributions

†These authors contributed equally (K.B.F. and D.B.G.).

Notes

The authors declare no competing financial interest.

■ ACKNOWLEDGMENTS

This work was financed by FEDER funds through COMPETE (Programa Operacional Factores de Competitividade) and by Portuguese funds through FCT (Fundação para a Ciência e a Tecnologia), in the framework of the Projects Pest-C/SAU/LA0002/2011 and BIOMATRIX (PTDC/SAU-BEB/101235/

2008 and FCOMP-01-0124-FEDER-010915). The authors C.C.B., S.G.S., and K.B.F. acknowledge Ciência 2008, Ciência 2007, and CAPES (Coordenação de Aperfeiçoamento de Pessoal de Nível Superior, BEX 5559-10-3), respectively, and funding from FLAD (Fundação Luso Americana) for in vivo studies. D.J.M. also acknowledges funding from NIH (R37 DE013033) for in vivo studies. The authors are grateful to Bidarra, S., Salgado, C., Vasconcelos, D., and Nascimento, D. for their participation in the blind test, Silva, D. from CEMUP (Centro de Materiais da Universidade do Porto) for the cryoSEM analyzes, and to Maia, F. R. for her help during manuscript preparation.

REFERENCES

(1) Vo, T. N.; Kasper, F. K.; Mikos, A. G. Strategies for controlled delivery of growth factors and cells for bone regeneration. *Adv. Drug Delivery Rev.* **2012**, *64*, 1292−1309.

(2) Tibbitt, M. W.; Anseth, K. S. Hydrogels as extracellular matrix mimics for 3D cell culture. *Biotechnol. Bioeng.* **2009**, *103*, 655−663.

(3) Bidarra, S. J.; Barrias, C. C.; Fonseca, K. B.; Barbosa, M. A.; Soares, R. A.; Granja, P. L. Injectable in situ crosslinkable RGD-modified alginate matrix for endothelial cells delivery. *Biomaterials* **2011**, *32*, 7897−7904.

(4) Salgado, C. L.; Sanchez, E. M. S.; Zavaglia, C. A. C.; Almeida, A. B.; Granja, P. L. Injectable biodegradable polycaprolactone−sebacic acid gels for bone tissue engineering. *Tissue Eng., Part A* **2011**, *18*, 137−146.

(5) Silva, E. A.; Mooney, D. J. Spatiotemporal control of vascular endothelial growth factor delivery from injectable hydrogels enhances angiogenesis. *J. Thromb. Haemostasis* **2007**, *5*, 590−598.

(6) Munarin, F.; Petrini, P.; Tanzi, M. C.; Barbosa, M. A.; Granja, P. L. Biofunctional chemically modified pectin for cell delivery. *Soft Matter* **2012**, *8*, 4731−4739.

(7) Haines-Butterick, L.; Rajagopal, K.; Branco, M.; Salick, D.; Rughani, R.; Pilarz, M.; Lamm, M. S.; Pochan, D. J.; Schneider, J. P. Controlling hydrogelation kinetics by peptide design for three-dimensional encapsulation and injectable delivery of cells. *Proc. Natl. Acad. Sci. U.S.A.* **2007**, *104*, 7791−7796.

(8) Yu, L.; Ding, J. Injectable hydrogels as unique biomedical materials. *Chem. Soc. Rev.* **2008**, *37*, 1473−1481.

(9) Oliveira, S. M.; Barrias, C. C.; Almeida, I. F.; Costa, P. C.; Ferreira, M. R. P.; Bahia, M. F.; Barbosa, M. A. Injectability of a bone filler system based on hydroxyapatite microspheres and a vehicle with in situ gel-forming ability. *J. Biomed. Mater. Res., Part B* **2008**, *87B*, 49−58.

(10) West, J. L.; Hubbell, J. A. Polymeric biomaterials with degradation sites for proteases involved in cell migration. *Macromolecules* **1999**, *32*, 241−244.

(11) Wang, C.; Varshney, R. R.; Wang, D. A. Therapeutic cell delivery and fate control in hydrogels and hydrogel hybrids. *Adv. Drug Delivery Rev.* **2010**, *62*, 699−710.

(12) Gustafson, J. A.; Price, R. A.; Frandsen, J.; Henak, C. R.; Cappello, J.; Ghandehari, H. Synthesis and characterization of a matrix-metalloproteinase responsive silk−elastinlike protein polymer. *Biomacromolecules* **2013**, *14*, 618−625.

(13) Lévesque, S. G.; Shoichet, M. S. Synthesis of enzyme-degradable, peptide-cross-linked dextran hydrogels. *Bioconjugate Chem.* **2007**, *18*, 874−885.

(14) Lutolf, M. P.; Hubbell, J. A. Synthetic biomaterials as instructive extracellular microenvironments for morphogenesis in tissue engineering. *Nat. Biotechnol.* **2005**, *23*, 47−55.

(15) Anderson, S. B.; Lin, C.-C.; Kuntzler, D. V.; Anseth, K. S. The performance of human mesenchymal stem cells encapsulated in cell-degradable polymer-peptide hydrogels. *Biomaterials* **2011**, *32*, 3564−3574.

(16) Giri, T. K.; Thakur, D.; Alexander, A.; Ajazuddin; Badwaik, H.; Tripathi, D. K. Alginate based hydrogel as a potential biopolymeric carrier for drug delivery and cell delivery systems: present status and applications. *Curr. Drug Delivery* **2012**, *9*, 539−555.

(17) Fonseca, K. B.; Bidarra, S. J.; Oliveira, M. J.; Granja, P. L.; Barrias, C. C. Molecularly designed alginate hydrogels susceptible to local proteolysis as three-dimensional cellular microenvironments. *Acta Biomater.* **2011**, *7*, 1674−1682.

(18) Fonseca, K. B.; Maia, F. R.; Cruz, F. A.; Andrade, D.; Juliano, M. A.; Granja, P. L.; Barrias, C. C. Enzymatic, physicochemical and biological properties of MMP-sensitive alginate hydrogels. *Soft Matter* **2013**, *9*, 3283−3292.

(19) Babensee, J. E. Interaction of dendritic cells with biomaterials. *Semin. Immunol.* **2008**, *20*, 101−108.

(20) Park, J.; Babensee, J. E. Differential functional effects of biomaterials on dendritic cell maturation. *Acta Biomater.* **2012**, *8*, 3606−3617.

(21) Babensee, J. E.; Paranjpe, A. Differential levels of dendritic cell maturation on different biomaterials used in combination products. *J. Biomed. Mater. Res., Part A* **2005**, *74A*, 503−510.

(22) Bouhadir, K. H.; Lee, K. Y.; Alsberg, E.; Damm, K. L.; Anderson, K. W.; Mooney, D. J. Degradation of partially oxidized alginate and its potential application for tissue Eengineering. *Biotechnol. Prog.* **2001**, *17*, 945−950.

(23) Evangelista, M. B.; Hsiong, S. X.; Fernandes, R.; Sampaio, P.; Kong, H.-J.; Barrias, C. C.; Salema, R.; Barbosa, M. A.; Mooney, D. J.; Granja, P. L. Upregulation of bone cell differentiation through immobilization within a synthetic extracellular matrix. *Biomaterials* **2007**, *28*, 3644−3655.

(24) Rowley, J. A.; Madlambayan, G.; Mooney, D. J. Alginate hydrogels as synthetic extracellular matrix materials. *Biomaterials* **1999**, *20*, 45−53.

(25) Oliveira, M. I.; Santos, S. G.; Oliveira, M. J.; Torres, A. L.; Barbosa, M. A. Chitosan drives anti-inflammatory macrophage polarisation and pro-inflammatory dendritic cell stimulation. *Eur. Cells Mater.* **2012**, *24*, 136−153.

(26) Chapuis, F.; Rosenzwajg, M.; Yagello, M.; Ekman, M.; Biberfeld, P.; Gluckman, J. C. Differentiation of human dendritic cells from monocytes in vitro. *Eur. J. Immunol.* **1997**, *27*, 431−441.

(27) Sallusto, F.; Lanzavecchia, A. Efficient presentation of soluble antigen by cultured human dendritic cells is maintained by granulocyte/macrophage colony-stimulating factor plus interleukin 4 and down-regulated by tumor necrosis factor alpha. *J. Exp. Med.* **1994**, *179*, 1109−1118.

(28) Santos, S.; Lynch, S.; Campbell, E.; Antoniou, A.; Powis, S. Induction of HLA-B27 heavy chain homodimer formation after activation in dendritic cells. *Arthritis Res. Ther.* **2008**, *10*, R100.

(29) Verhasselt, V.; Buelens, C.; Willems, F.; De Groote, D.; Haeffner-Cavaillon, N.; Goldman, M. Bacterial lipopolysaccharide stimulates the production of cytokines and the expression of costimulatory molecules by human peripheral blood dendritic cells: evidence for a soluble CD14-dependent pathway. *J. Immunol.* **1997**, *158*, 2919−2125.

(30) Joffre, O.; Nolte, M. A.; Spörri, R.; Sousa, C. R. Inflammatory signals in dendritic cell activation and the induction of adaptive immunity. *Immunol. Rev.* **2009**, *227*, 234−247.

(31) Banchereau, J.; Steinman, R. M. Dendritic cells and the control of immunity. *Nature* **1998**, *392*, 245−252.

(32) Engler, A. J.; Sen, S.; Sweeney, H. L.; Discher, D. E. Matrix elasticity directs stem cell lineage specification. *Cell* **2006**, *126*, 677−689.

(33) Koski, G. K.; Koldovsky, U.; Xu, S.; Mick, R.; Sharma, A.; Fitzpatrick, E.; Weinstein, S.; Nisenbaum, H.; Levine, B. L.; Fox, K.; Zhang, P.; Czerniecki, B. J. A novel dendritic cell-based immunization approach for the induction of durable Th1-polarized anti-HER-2/neu responses in women with early breast cancer. *J. Immunother.* **2012**, *35*, 54−65.

(34) Bajpai, S. K.; Sharma, S. Investigation of swelling/degradation behaviour of alginate beads crosslinked with Ca^{2+} and Ba^{2+} ions. *React. Funct. Polym.* **2004**, *59*, 129−140.

(35) Alsberg, E.; Kong, H. J.; Hirano, Y.; Smith, M. K.; Albeiruti, A.; Mooney, D. J. Regulating bone formation via controlled scaffold degradation. *J. Dent. Res.* **2003**, *82*, 903−908.

(36) Chau, Y.; Luo, Y.; Cheung, A. C.; Nagai, Y.; Zhang, S.; Kobler, J. B.; Zeitels, S. M.; Langer, R. Incorporation of a matrix metalloproteinase-sensitive substrate into self-assembling peptides: a model for biofunctional scaffolds. *Biomaterials* **2008**, *29*, 1713−1719.

(37) Ries, C.; Egea, V.; Karow, M.; Kolb, H.; Jochum, M.; Neth, P. MMP-2, MT1-MMP, and TIMP-2 are essential for the invasive capacity of human mesenchymal stem cells: differential regulation by inflammatory cytokines. *Blood* **2007**, *109*, 4055−4063.
(38) Bott, K.; Upton, Z.; Schrobback, K.; Ehrbar, M.; Hubbell, J. A.; Lutolf, M. P.; Rizzi, S. C. The effect of matrix characteristics on fibroblast proliferation in 3D gels. *Biomaterials* **2010**, *31*, 8454−8464.
(39) Ehrbar, M.; Sala, A.; Lienemann, P.; Ranga, A.; Mosiewicz, K.; Bittermann, A.; Rizzi, S. C.; Weber, F. E.; Lutolf, M. P. Elucidating the role of matrix stiffness in 3D cell migration and remodeling. *Biophys. J.* **2011**, *100*, 284−293.
(40) Bidarra, S. l. J.; Barrias, C. C.; Barbosa, M. A.; Soares, R.; Granja, P. L. Immobilization of human mesenchymal stem cells within RGD-grafted alginate microspheres and assessment of their angiogenic potential. *Biomacromolecules* **2010**, *11*, 1956−1964.